A New Model of Dark Energy EoS : Constrains on Free Parameters & Related Cosmological Parameters

Promila Biswas[1] and *Ritabrata Biswas*[2]

Department of Mathematics, The University of Burdwan, Golapbag Academic Complex, City : Burdwan-713104, District : Purba Bardhaman, State : West Bengal, Country : India.

Abstract

Since the Ia supernovae observations of late 1990's, it has been predicted that our universe is experiencing a late time cosmic acceleration. To build a theoretical support to this observation, the existence of hypothetical fluid inside the universe is assumed which exerts negative pressure. Several candidates of such an exotic fluid have been prescribed so far. A popular method in this alley is to parametrize the equation of state parameter $\omega = \frac{p}{\rho}$ as a function of redshift. Again some common families of such redshift parametrizations are constructed of which different members have given different properties of universe. Mainly, these were model dependent studies where free parameters are to be constrained by different observations. In the present article, we have considered a new expression for redshift parametrization and have constrained its free parameters for two Hubble parameter vs redshift data sets. These two data sets are obtained depending on two basic methodologies known as differential ages method and baryonic acoustic oscillation method. We locate different confidence contours for our model under the constraints of these two data sets. Besides, we analyse different thermodynamic parameters related to the evolution of our universe. It is noticed that our model indicates towards a delayed dark matter decay model which mimics EoS=-1 phenomena at the present epoch. We study the deceleration parameters behaviors. We compare the outcomes for both the data sets.

1 Introduction

Twenty years ago from now, the late time cosmic acceleration was pointed out by the observations of two independent supernova observation collaborating teams [1, 2]. This has speculated the cosmic solution comprised of time independent, spatially homogeneous hypothetical matter density and constant positive space curvature. It led us to the establishment of cosmological constant model (with $\Omega_m \approx 0.3$, $\Omega_\Lambda \approx 0.7$) as the preferred alternative to the $\Omega_m = 1$ scenario. To build the first cosmological model, Albert Einstein in the reference [3], introduced a constant term (Λ) to his field equations of General Relativity (GR). One can view "Cosmological Constant" as a constant valued energy density of the vacuum [4]. This term did appear as an unnecessary one, once the dynamic cosmological models [5, 6] were evolved and cosmic expansion was discovered [7]. The repulsive gravitational effects of such energy balance the attractive nature of gravity of matter and thereby allow a static cosmological solution. Soon after this, CMB evidence for a spatially flat universe [8, 9], the proposition for $\Omega_{tot} \approx 1$ was declared. This did fully eliminate the free expansion alternative with $\Omega_m << 1$, $\Omega_\lambda = 0$. The scale factor $a(t)$, governed by GR grows at an accelerating rate if the pressure, $p < -\frac{1}{3}\rho$. It is a popular methodology to introduce a hypothetical fluid/energy component which exerts negative pressure to the right hand side of Einstein's field equations and to use such a model to explain the late time cosmic acceleration. The name of such exotic matter is coined as quintessence, phantom or dark energy (DE). The value of equation of state (EoS) of such fluids ($\omega = \frac{p}{\rho}$) is taken to be negative [10, 11]. Most natural existence of this kind of energy density can be simply obtained by reintroducing the cosmological constant term Λ into Einstein's field equations. The cosmological upper bound ($\rho_a \lesssim 10^{71}GeV^4$) by more than the order of hundreds is satisfied if this particular DE interpretation of cosmological constant is entertained [11]. Flat ΛCDM model with $\Omega_{tot} = 1$ or ωCDM models are famous (ω is the EoS parameter of DE). Though Λ is well equipped with the explanations of majority of the observational evidence regarding cosmic acceleration (if DE is assumed to be associated with the vacuum energy

---

density), we search for a better model to reduce the huge discrepancies between observation and theory. Amongst them, the time varying cosmological constant term model [12], irreversible process of cosmological matter creation [13], Chaplygin gas family [14], redshift parametrization of the EoS parameters [15, 16] etc are familiar ones. Scalar field ϕ with potential $V(\phi)$ [17] is proposed as another model which acts like cosmological constant in the limit $\frac{1}{2} << |V(\phi)|$. The value of the EoS for scalar field, $\omega_\phi = \frac{p_\phi}{\rho_\phi}$, evolves with time in a way that depends on $V(\phi)$ and on initial conditions $(\phi_i, \dot{\phi}_i)$.

The expansion rate of the universe, $H(z)$, governed by Friedmann equation, for DE EoS $\omega(z)$, gives the evolution of DE density as

$$\Omega_{DE}\frac{\rho_{DE}(z)}{\rho_{DE}(z=0)} = \Omega_{DE}\ exp\left[3\int_0^z [1 + \omega(z')]\frac{dz'}{1+z'}\right] = \Omega_{DE}(1+z)^{3(1+\omega)} \qquad .$$

If the present values of Ω_m, Ω_λ and Ω_{tot} are known, the process of measuring $H(z)$ focusses on the values of $\omega(z)$ particularly. In GR based linear perturbation theory, the density contrast $\delta(\vec{x}, t) \equiv \frac{\rho(\vec{x},t)}{\rho(t)} - 1$ of pressureless matter grows in proportion to the linear growth function $G(t)$, which is followed by the differential equation

$$\ddot{G} + 2H(z)\dot{G} - \frac{3}{2}\Omega_m H_0^2(1+z)^3 G = 0 \qquad ,$$

where "." means differentiation with respect to t.

Upto a good approximation, the logarithmic derivative of $G(z)$ is

$$f(z) \equiv -\frac{dlnG}{dln(1+z)} \approx \left[\Omega_m(1+z)^3\frac{H_0^2}{H^2(z)}\right]^\gamma \qquad ,$$

where $\gamma \approx 0.55$ for relevant values of cosmological parameters [18]. Oscillations in $\omega(z)$ over a range $\frac{\Delta z}{1+z} << 1$ are therefore extremely difficult to constrain. There exists convention is there to phase constrain $\omega(z)$ in terms of linear evolution model, $\omega(a) = \omega_0 + \omega_a(1 - a) = \omega p + \omega_a(a_p - a)$, where $a = \frac{1}{1+z}$, ω_0 is the value of ω at $z = 0$, and ω_p is the value of ω at a pivot redshift $z_p = a_p^{-1} - 1$. A widely used figure of merit (FOM) for DE experiments [19] is the projected combination of errors $[\sigma(\omega_p)\sigma(\omega_a)]^{-1}$. A richer description (up to $0.1 - 0.3\%$) of $\omega(z)$ can be obtained in future.

More general set of cosmological parameters is constructed. The particular necessary parameters are :-

(i) The dimensionless Hubble's parameter $h = \frac{H_0}{100}kms^{-1}Mpc^{-1}$ which determines the present day value of the critical density and the overall scaling of distances inferred from redshifts.

(ii) Ω_m and Ω_{tot} affects the expansion history and distance redshift relation.

(iii) The sound horizon $r_s = \int_0^{t_{rec}} c_s(t)\frac{dt}{a(t)}$, the comoving distance that pressure waves can propagate between $t = 0$ and recombination, determines the physical scale of the acoustic peaks in the CMB [21] and the baryon acoustic oscillations (BAO) feature in low redshift matter clustering [22].

(iv) The amplitude of matter fluctuations, conventionally represented by the quantity $\sigma_8(z)$, scales the overall amplitude of growth measurements such as weak lensing or redshift-space distortions.

Redshift parametrizations of DE EoS is a time dependent modelling and can not be obtained from the scalar field dynamics as these are not limited functions, i.e., they do not lie in the interval defined by $\omega = \frac{\frac{\dot{\phi}^2}{2} - V(\phi)}{\frac{\dot{\phi}^2}{2} + V(\phi)}$, where $V(\phi)$ is the field potential. Two prior families of redshift parametrizations are

family I : $\omega(z) = \omega_0 + \omega_1\left(\frac{z}{1+z}\right)^n$ and

family II : $\omega(z) = \omega_0 + \omega_1\frac{z}{(1+z)^n}$, $\mathbf{n} \in \mathbb{N}$.

Some other redshift parametrization of DE EoS members such as Barboza-Alcaniz [59], Efstathiou parametrization [60, 61], ASSS parametrization [62, 63], Hannestad Mörtsell Parametrization [64], Lee Parametrization [65], Feng Shen Li Li (FSLL) Parametrization [66], Polynomial Parametrization [67, 68].

In this article, our motivation is to propose a new EoS for DE which behaves better than other models and creates $\omega(z) = -1$ epoch at $z = 0$. General trend of a model dependent study of cosmology done by constraining the free parameters. In this article, we wish to propose a new redshift parameterization for DE EoS and constrain it under two different data sets. While proposing the DE EoS we take care that it does not fall in any of family I or family II. The model has completely a new structure depending on redshift z. We will try to show whether the our model generates $\omega(z) = -1$ epoch in the neighbourhood of $z = 0$ or not. We wish to study the nature of fractional dimensionless

density parameters for our model. We plan to study the behaviour of the deceleration parameter $q(z)$ for the proposed model and whether phase transition-(s) from deceleration to acceleration or the converse take(s) place or not.

The article is organised as follows : In section 2 we construct the cosmological model for our newly proposed parameterization. In section 3 we constrain the model under the data sets obtained with the help of differential ages method and Baryonic Acoustic Oscillation method. Section 4 comprises of studies of different cosmological parameters related to our model. Finally, we briefly discuss our findings and conclude in the last section.

2 Mathematical Modelling of a New Kind of Redshift Parametrization

In FLRW space time, Einstein's field equations (with flat spatial section) can be described as

$$3\frac{\dot{a}^2}{a^2} = \rho_m + \frac{1}{2}\dot{\phi}^2 + V(\phi) = \rho_m + \rho_\phi \tag{1}$$

and

$$2\frac{\ddot{a}}{a} + \frac{\dot{a}^2}{a^2} = -\frac{1}{2}\dot{\phi}^2 + V(\phi) = -p_\phi \qquad , \tag{2}$$

where $8\pi G = c = 1$, ϕ is the scalar field in natural units, ρ_m is the matter density, ρ_ϕ is the density of scalar field, p_ϕ is the pressure of the scalar field, V is the scalar field potential.

The energy density ρ_ϕ and pressure p_ϕ should have the structures as

$$\rho_\phi = \frac{1}{2}\dot{\phi}^2 + V(\phi) \qquad and \qquad p_\phi = \frac{1}{2}\dot{\phi}^2 - V(\phi) \qquad . \tag{3}$$

Then the conservation equations for non interactive DE - dark matter (DM) are given as follows,

$$for\ energy \qquad \dot{\rho_\phi} + 3H(\rho_\phi + p_\phi) = 0 \tag{4}$$

and

$$for\ matter \qquad \dot{\rho_m} + 3H\rho_m = 0 \Rightarrow \rho_m = \rho_{m0}a^{-3} \qquad , \tag{5}$$

where ρ_{m0} is the current value of energy density for matter field. Equation (4) can be rewritten as

$$\omega_\phi = \frac{p_\phi}{\rho_\phi} = -1 - \frac{a}{3\rho_\phi}\frac{d\rho_\phi}{da} \tag{6}$$

Among the above equations (1), (2), (4) and (5), only three equations are likely to be independent to each other. Bianchi identities can show the derivation of fourth equation. So, we are going to solve for four independent variables. Without an additional input, it is impossible to find an exact solution. We propose an ansatz for the functional form of ρ_ϕ as

$$\frac{1}{\rho_\phi}\frac{d\rho_\phi}{da} = -3\left[\frac{\lambda_1}{1+ak_1} + \frac{\lambda_2(1-a)}{(1+ak_2)^2}\right] \qquad , \tag{7}$$

where λ_1, λ_2, k_1 and k_2 are constants.

Integrating, we get

$$\rho_\phi = A(1+ak_1)^{-\frac{3\lambda_1}{k_1}}(1+ak_2)^{\frac{3\lambda_2}{k_2^2}}exp\left\{\frac{3\lambda_2(1+k_2)}{k_2^2(1+ak_2)}\right\} \qquad , \tag{8}$$

where $A = \rho_{\phi 0}(1+k_1)^{\frac{3\lambda_1}{k_1}}(1+k_2)^{-\frac{3\lambda_2}{k_2^2}}exp\left\{-\frac{3\lambda_2}{k_2^2}\right\}$ and $\rho_{\phi 0}$ is the present time (at $z = 0$) value of the scalar field density. We observe that the density is depending on three distinct functions of a. If we make $\lambda_2 = 0$ and $k_1 = 1$, we see the solution will take a simple power law evolution of $\rho_\phi(\sim a^{-\lambda})$, considered in many cosmological studies [23]. Equations (7) and (8) together give us the EoS parameter ω_ϕ as a function of redshift ($z = \frac{1}{a} - 1$) as

$$\omega_\phi(z) = -1 + \frac{\lambda_1}{(1+k_1)+z} + \frac{\lambda_2 z}{\{(1+k_2)+z\}^2} \tag{9}$$

This equation even can be treated to be same of

$$\omega_\phi(z) = \omega_0 + \frac{\omega_1}{\omega_2 + z} + \frac{\omega_3 z}{(\omega_4 + z)^2} \tag{10}$$

In the next section we will constrain two of the free parameters of our model, namely, λ_1 & λ_2 by the help of Hubble's parameter vs redshift data.

3 Constraining the Free Parameters for DA and BAO method :

Equation (10) depicts a new construction of DE equation of state parameter. From (1), (5) and (9) we have

$$H^2 = H_0^2 \left[\Omega_{rad,0} a^{-4} + \Omega_{m0} a^{-3} + \Omega_{\phi,0} \beta (1 + a k_1)^{-\frac{3\lambda_1}{k_1}} (1 + a k_2)^{\frac{3\lambda_2}{k_2^2}} exp \left\{ \frac{3\lambda_2(1 + k_2)}{k_2^2(1 + a k_2)} \right\} \right] \qquad , \qquad (11)$$

where $\beta = (1 + k_1)^{\frac{3\lambda_1}{k_1}} (1 + k_2)^{-\frac{3\lambda_2}{k_2^2}} exp\{-\frac{3\lambda_2}{k_2^2}\}$ is a constant and $\Omega_{m0} = \frac{\rho_{m0}}{3H_0^2}$, $\Omega_{rad,0} = \frac{\rho_{rad,0}}{3H_0^2}$ and $\Omega_{\phi 0} = \frac{\rho_{\phi 0}}{3H_0^2} = 1 - \Omega_{rad,0} - \Omega_{m0}$ represent the current values of the dimensionless density parameters for the matter, radiation and the scalar field respectively. Now we will proceed for constraining the parametrization free parameters with Hubble parameter vs redshift data. For this we must enlist the data first and mention the methods for collecting the data.

While we look through the sky, if the distance through which we see some object is shorter one, Cepheid variables are used as standard candles. For distant galaxies, type Ia supernova explosions (SNeIa) are taken as standard candles [1, 2]. As a standard ruler, we use the measurements of fluctuations in the visible baryonic matter's density caused by acoustic density waves in early universe's primordial plasma [24, 25]. This standard ruler's length is given by the maximum distance an acoustic wave could travel through the primordial plasma until the plasma is cooled to the point where it turns to neutral atoms. This oscillation is known as baryon acoustic oscillations (BAO). Alongwith the mentioned candles and rulers, study of Cosmic Microwave Background (CMB) [26] has strengthen the studies of expanding universe since last twenty years. CMB is the remnant electromagnetic radiation which came out of early Big Bang cosmology. The developments of standard ΛCDM cosmological model is done. These methodologies, however, do not directly constrain the Hubble's parameter. An independent methodology to constrain the history of the universe's expansion is done by "cosmic chronometer" [27, 28] approach. This method states a measurement of the expansion rate without relying on the nature of the metric between the chronometer and us. This is not the case for methods which depends on integrated quantities along the line of sight [27, 28].

An analysis of the sample of $\sim$ 11,000 massive and passive galaxies are done and eight measurements of the Hubble parameter have been enlisted with an accuracy of 5-12% in the redshift range $0.15 < z < 1.1$ in the reference [29]. For low redshifts ($z < 0.3$), most of the accurate constraints were found. Cosmic chronometers method and standard probe's (like SNeIa and BAO) comparative discussions are found in the references [30, 31, 19, 32]. In the reference [33], some more $H(z)$ points for the redshift range $0.35 < z < 0.5$ are enlisted.

We can speculate a star's age by the analysis of spectra coming out of it. On a cosmic scale, we can take the ensembles of stars, i.e., galaxies to point out the ages. This study presents a clock's behaviour in front of us. "This so called clock" can be found in archival data [34], Gemini Deep Deep Survey (GDDS) [35], In the size method, the BAO signature density auto-correlation function can be used as the "standard rod". This whole theory is standing on the believe that almost all the stars of a galaxy are formed of a single 'burst' [36].

In differential ages (DA) method we can find more sensitive results for $\omega(z)$. In this method, we have to keep belief on a clock, the dates of which may vary in the age of the universe with redshift. The clock is provided by spectroscopic dating of galaxy's ages. We can infer the derivative ($\frac{dz}{dt}$) from $\frac{\triangle z}{\triangle t}$ ratio as based on $\triangle t$ and $\triangle z$, where $\triangle t$ is measurement of age difference and between two passively turned up galaxies that formed at the same time but they are separated by $\triangle z$ (a small redshift interval). This method is more reliable than an absolute age determination method for galaxies [37, 38, 39]. The case of globular clusters, absolute stellar ages are more permeable to well connected ages. Moreover, we can obtain only the lower limit to the age of the universe from absolute galaxy ages and place weak constraints of $\omega(z)$.

The quantity measured related to Hubble parameter

$$H(z) = -\frac{1}{(1 + z)} \frac{dz}{dt} \Rightarrow \frac{dt}{dz} = -\frac{1}{H(z)(1 + z)}$$

Applying this method to old galaxies (which are elliptical in the local universe) one can evaluate H_0 (the current value of Hubble constant).

Now we will enlist $H(z)$ vs z values and the corresponding error terms using DA method in Table I. Measurements of $H(z)$ using the standard ruler provided by BAO method are given in table II.

Table-I : Hubble parameter $H(z)$ with redshift and errors σ_H from DA method

Sl No.	z	$H(z)$	$\sigma(z)$	Ref. No.	Sl No.	z	$H(z)$	$\sigma(z)$	Ref. No.
1	0	67.77	1.30	[40]	24	0.4783	80.9	9	[33]
2	0.07	69	19.6	[41]	25	0.48	97	60	[43]
3	0.09	69	12	[42]	26	0.51	90.4	1.9	[46]
4	0.1	69	12	[43]	27	0.57	96.8	3.4	[49]
5	0.12	68.6	26.2	[41]	28	0.593	104	13	[29]
6	0.17	83	8	[43]	29	0.6	87.9	6.1	[47]
7	0.179	75	4	[29]	30	0.61	97.3	2.1	[46]
8	0.1993	75	5	[28, 29]	31	0.68	92	8	[29]
9	0.2	72.9	29.6	[41]	32	0.73	97.3	7	[47]
10	0.24	79.7	2.7	[44]	33	0.781	105	12	[29]
11	0.27	77	14	[43]	34	0.875	125	17	[29]
12	0.28	88.8	36.6	[41]	35	0.88	90	40	[43]
13	0.35	82.7	8.4	[45]	36	0.9	117	23	[43]
14	0.352	83	14	[29]	37	1.037	154	20	[29]
15	0.38	81.5	1.9	[46]	38	1.3	168	17	[43]
16	0.3802	83	13.5	[33]	39	1.363	160	33.6	[50]
17	0.4	95	17	[42]	40	1.43	177	18	[43]
18	0.4004	77	10.2	[33]	41	1.53	140	14	[43]
19	0.4247	87.1	11.2	[33]	42	1.75	202	40	[43]
20	0.43	86.5	3.7	[44]	43	1.965	186.5	50.4	[50]
21	0.44	82.6	7.8	[47]	44	2.3	224.0	8.0	[51]
22	0.44497	92.8	12.9	[33]	45	2.34	222	7	[52]
23	0.47	89	49.6	[28, 48]	46	2.36	226	8	[53]

Table-II : Hubble parameter $H(z)$ with redshift and errors σ_H from BAO method

Sl No.	z	$H(z)$	$\sigma(z)$	Ref. No.	Sl No.	z	$H(z)$	$\sigma(z)$	Ref. No.
1	0.24	79.69	2.99	[44]	14	0.52	94.35	2.64	[55]
2	0.30	81.7	6.22	[54]	15	0.56	93.34	2.3	[55]
3	0.31	78.18	4.74	[55]	16	0.57	87.6	7.8	[57]
4	0.34	83.8	3.66	[44]	17	0.57	96.8	3.4	[49]
5	0.35	82.7	9.1	[56]	18	0.59	98.48	3.18	[55]
6	0.36	79.94	3.38	[55]	19	0.60	87.9	6.1	[47]
7	0.38	81.5	1.9	[46]	20	0.61	97.3	2.1	[46]
8	0.40	82.04	2.03	[55]	21	0.64	98.82	2.98	[55]
9	0.43	86.45	3.97	[44]	22	0.73	97.3	7.0	[47]
10	0.44	82.6	7.8	[47]	23	2.30	224	8.6	[51]
11	0.44	84.81	1.83	[55]	24	2.33	224	8 7	[58]
12	0.48	87.79	2.03	[55]	25	2.34	222	8.5	[52]
13	0.51	90.4	1.9	[46]	26	2.36	226	9.3	[53]

Using the above data for both methods, we will plot $H(z) - z$ graphs in figure 1.

We can see the values of $H(z)$ corresponding to the values of redshift z are semi increasing. So the resultant graph increases with respect to z. For lower redshift, BAO method estimates the higher values of $H(z)$ than DA method. Again, for higher redshift, DA method determines the higher values of $H(z)$ as compared to BAO method. Now we will constrain our model's parameters given in equation (10) with the help of the data of table I and II.

In fig.2(a), we have plotted the best fit values for λ_1 and λ_2 along with their corresponding 1σ, 2σ, 3σ confidence contours using the datasets from table I and table II respectively. Figure 2(b) uses BAO with the data sets to constrain λ_1 and λ_2. BAO and CMB along with the data sets are given figure 2(c). First we will analyse fig 2(a). For DA method, the point of best fit is denoted by "P" and 1σ, 2σ, 3σ confidence regions are drawn in red, blue and black dashed lines respectively. For BAO method, "Q" is the best fit and the regions coloured as green, brown and red solid lines for 1σ, 2σ, 3σ confidence contours respectively.

For both the datasets the confidence regions are of more or less elliptic structure and the semi major axis for the regions have the slope more than a right angle. However, slope of confidence contours for DA method is higher than that of BAO method. Tendency wise, high λ_1 is supported with low λ_2 to stay in to particular confidence region whereas low value of λ_1 is accompanied with high λ_2. This signifies the DE model given in equation (9) allows either
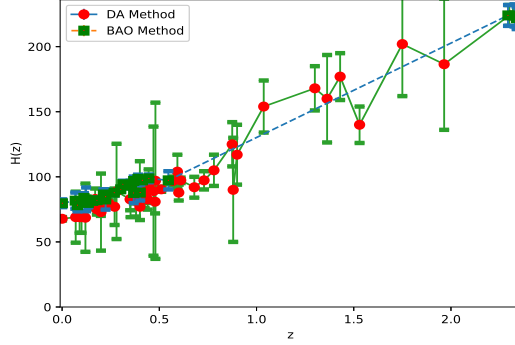
Fig. 1 : $H(z) - z$ graph using the dataset from table I and II. Red circle and green rectangle symbol indicate DA method and BAO method respectively.
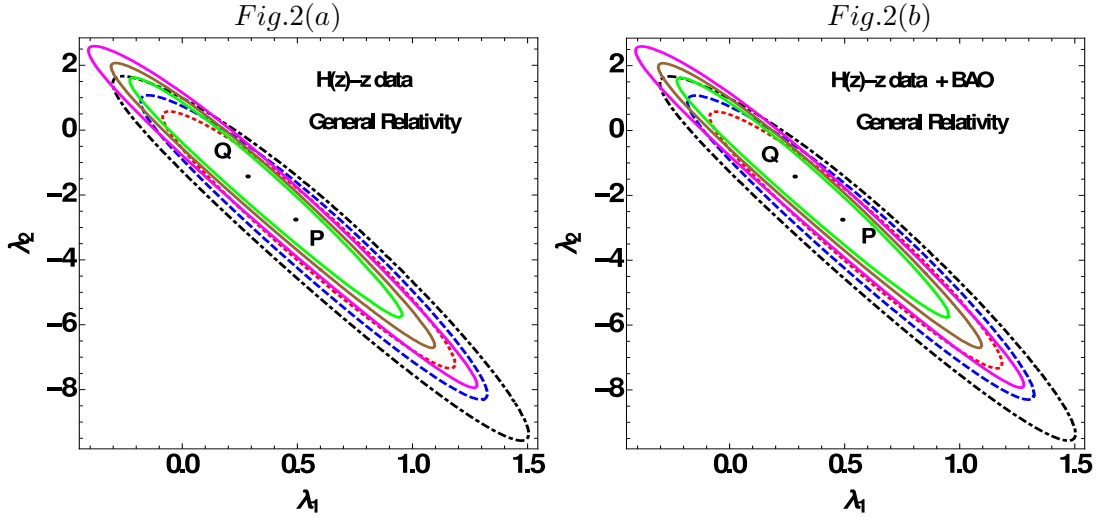

Fig.2(a)-(b) : 1σ, 2σ, 3σ confidence contours for $H(z) - z$ dataset and $H(z) - z + $ BAO dataset

of the second or third term to dominate. At the best fits, if we take $z = 0$, then $\omega(z) = -0.553388$ for DA method and $\omega(z) = -0.741869$ for BAO method. The spans of different regions for both cases are enlisted in table - III.

Comparison shows the length of major axis for confidence contours of or BAO data (table I) is less than that for DA data (table II). So lesser amount of region is enclosed as 1σ confidence if we consider BAO method. The maximum portion of 1σ region of BAO is common to that of DA. So BAO method has the tendency to constrain the parameters.

BAO peak parameter is proposed by the reference [24]. SDSS survey detected BAO signal at a scale of $\sim 100 MPc$. For our redshift parametrization model, we will investigate the values of λ_1 and λ_2 using the BAO peak joint analysis. We will run this process for $0 < z < z_1$, where $z_1 = 0.236$. While SDSS data samples are considered, z_1 is called the typical redshift [70]. BAO peak parameter is defined as

$$\mathcal{A}_{BAO} = \frac{\sqrt{\Omega_m}}{E(z_1)^{\frac{1}{3}}} \left(\frac{\int_0^{z_1} \frac{dz}{E(z)}}{z_1} \right)^{\frac{2}{3}}$$

The value of $\mathcal{A}_{BAO}$ is 0.469 ± 0.017 for flat FLRW model. Hence, for analysis, the χ^2_{BAO} can be written in the form

$$\chi^2_{BAO} = \frac{(\mathcal{A}_{BAO} - 0.469)^2}{0.017^2}$$

We have drawn the figure 2(b) for $H(z) - z$ data set along with BAO constraint. The addition of BAO does not change the basic nature of the confidence contours. The best fits and the stretch of regions are enlisted are in table IV. At $z = 0$, according to the best fits, $\omega(z)$ should be -0.554712 for DA method and -0.742965 for BAO method.
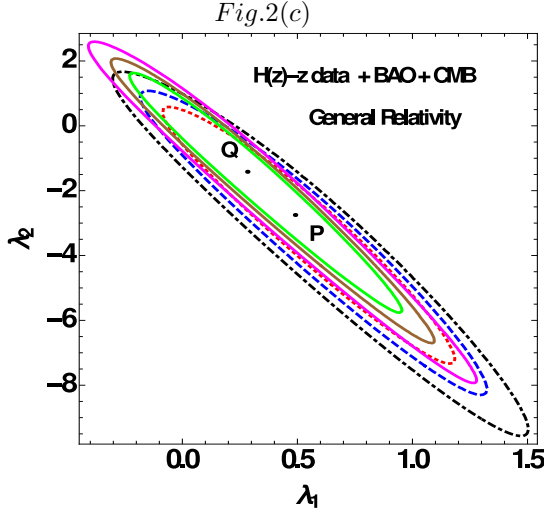
6

Fig.2(c)

H(z)−z data + BAO + CMB

General Relativity

Fig.2(c) : 1σ, 2σ, 3σ confidence contours for $H(z) - z$ dataset + BAO + CMB

The shift parameter of CMB power spectrum peak is given by [71, 72]

$$\mathcal{R} = \sqrt{\Omega_m} \int_0^{z_2} \frac{dz'}{E(z')}$$

where z_2 denotes the value of the redshift at the last scattering surface. WMAP predicts the value of $\mathcal{R} = 1.726 \pm 0.018$ at the redshift $z = 1091.3$. For CMB measurement, the χ^2_{CMB} function is defined as

$$\chi^2_{CMB} = \frac{(\mathcal{R} - 1.726)^2}{0.018^2}$$

We have imposed this method and have drawn the confidence contours in fig 2(c).

The best fits and the spans of confidence contours are given in the table V. Secondly, the best fits are placed in the fourth quadrant. In this case at present epoch ($z = 0$) the best fits $\omega(z) = -1$ for DA method and -0.743405 for BAO method.

We can predict that this cosmological model with BAO and CMB is the best measurement to match our result with ΛCDM model as we can see the value of $\omega(z = 0) = -1$ after using both BAO and CMB with $H(z) - z$ data in this model.

Table III :The best fit values of λ_1, λ_2, χ^2 and corresponding region of 1σ, 2σ and 3σ for both DA and BAO method using $H(z) - z$ data set

Tools	stat. info	Region of the contours			
		DA Method		BAO Method	
	Best fits	$\chi^2 = 44.3734$, $\omega(z)\big|_{z=0} = -0.553388$		$\chi^2 = 32.346$, $\omega(z)\big|_{z=0} = -0.741869$	
$H(z) - z$ data		$\lambda_1 = $ 0.491273 (V_{11})	$\lambda_2 = $ -2.75766 (V_{12})	$\lambda_1 = $ 0.283944 (V_{21})	$\lambda_2 = $ -1.42732 (V_{22})
	1σ	$V_{11}{}^{+0.704727}_{-0.587388}$	$V_{12}{}^{+3.38546}_{-4.64334}$	$V_{21}{}^{+0.679856}_{-0.52544}$	$V_{22}{}^{+3.10732}_{-4.42068}$
	2σ	$V_{11}{}^{+846727}_{-0.684273}$	$V_{12}{}^{+3.87666}_{-5.62634}$	$V_{21}{}^{+0.822056}_{-0.608144}$	$V_{22}{}^{+3.58232}_{-5.37068}$
	3σ	$V_{11}{}^{+1.021727}_{-0.800673}$	$V_{12}{}^{+4.49166}_{-6.85434}$	$V_{21}{}^{+1.005056}_{-0.702744}$	$V_{22}{}^{+4.09432}_{-6.61268}$

Table IV :The best fit values of λ_1, λ_2, χ^2 and corresponding region of 1σ, 2σ and 3σ for both DA and BAO method using $H(z) - z$ + BAO data set

Tools	stat. info	Region of the contours			
		DA Method		BAO Method	
	Best fits	$\chi^2 = 804.712$, $\omega(z)\big|_{z=0} = -0.554712$		$\chi^2 = 792.668$, $\omega(z)\big|_{z=0} = -0.742965$	
$H(z) - z$ data + BAO		$\lambda_1 = $ 0.489817 (V_{11})	$\lambda_2 = $ -2.75048 (V_{12})	$\lambda_1 = $ 0.282739 (V_{21})	$\lambda_2 = $ -1.4207 (V_{22})
	1σ	$V_{11}{}^{+7.06183}_{-0.590517}$	$V_{12}{}^{+3.373787}_{-4.614513}$	$V_{21}{}^{+0.681061}_{-0.524239}$	$V_{22}{}^{+3.1287}_{-4.4333}$
	2σ	$V_{11}{}^{+0.846183}_{-0.685317}$	$V_{12}{}^{+3.914487}_{-5.618513}$	$V_{21}{}^{+0.823261}_{-0.606939}$	$V_{22}{}^{+3.5347}_{-5.3553}$
	3σ	$V_{11}{}^{+1.025183}_{-0.794917}$	$V_{12}{}^{+4.454487}_{-6.853513}$	$V_{21}{}^{+1.006261}_{-0.701539}$	$V_{22}{}^{+4.0507}_{-6.5723}$

Table V :The best fit values of λ_1, λ_2, χ^2 and corresponding region of 1σ, 2σ and 3σ for both DA and BAO method using $H(z) - z$ + BAO + CMB data set

Tools	stat. info	Region of the contours			
		DA Method		BAO Method	
$H(z) - z$ data + BAO + CMB	Best fits	$\chi^2 = 9999.38$, $\omega(z)\big|_{z=0} = -1$		$\chi^2 = 9987.35$, $\omega(z)\big|_{z=0} = -0.743405$	
		$\lambda_1 =$ 0.489817 (V_{11})	$\lambda_2 =$ -2.75048 (V_{12})	$\lambda_1 =$ 0.282254 (V_{21})	$\lambda_2 =$ -1.4176 (V_{22})
	1σ	$V_{11}{}^{+0.700183}_{-0.582677}$	$V_{12}{}^{+3.38758}_{-4.63252}$	$V_{21}{}^{+0.523754}_{-0.681546}$	$V_{22}{}^{+3.0796}_{-4.4134}$
	2σ	$V_{11}{}^{+0.846183}_{-0.683817}$	$V_{12}{}^{+3.86148}_{-5.61952}$	$V_{21}{}^{+0.823746}_{-0.606454}$	$V_{22}{}^{+3.5146}_{-5.3554}$
	3σ	$V_{11}{}^{+1.016183}_{-0.803917}$	$V_{12}{}^{+4.41448}_{-6.88352}$	$V_{21}{}^{+1.006746}_{-0.701054}$	$V_{22}{}^{+4.0576}_{-6.5864}$

4 Studies of Different Cosmological Parameters of this Parameterization :

The deceleration parameter q is defined as

$$q = -\frac{\ddot{a}}{aH^2} = -\left(1 + \frac{\dot{H}}{H^2}\right) \tag{12}$$

where $\dot{H} = \frac{dH}{dt} = aH\frac{dH}{da}$.

From equations (11) and (12), the expression for q in terms of scale factor a can be written as,

$$q(a) = -1 + \frac{2\Omega_{rad,0}a^{-4} + \frac{3}{2}\Omega_{m0}a^{-3} - \frac{3a}{2}\beta\,\Omega_{\phi0}\,(1+ak_1)^{-\frac{3\lambda_1}{k_1}}(1+ak_2)^{\frac{3\lambda_2}{k_2^2}}exp\left\{\frac{3\lambda_2(1+k_2)}{k_2^2(1+ak_2)}\right\}}{\Omega_{rad,0}a^{-4} + \Omega_{m0}a^{-3} + \beta\,\Omega_{\phi0}\,(1+ak_1)^{-\frac{3\lambda_1}{k_1}}(1+ak_2)^{\frac{3\lambda_2}{k_2^2}}exp\left\{\frac{3\lambda_2(1+k_2)}{k_2^2(1+ak_2)}\right\}}$$

$$\times\left[\lambda_2\,(1+ak_2)^{-1} - \lambda_2\,(1+k_2)(1+ak_2)^{-2} - \lambda_1\,(1+ak_1)^{-1}\right] \qquad . \tag{13}$$

Now, the equation (13), in terms of redshift z is

$$q(z) = -1 + \frac{2\Omega_{rad,0}(1+z)^4 + \frac{3}{2}\Omega_{m0}(1+z)^3 - \frac{3}{2(1+z)}\Omega_{\phi0}\,\beta\,(\frac{1+k_1+z}{1+z})^{-\frac{3\lambda_1}{k_1}}(\frac{1+k_2+z}{1+z})^{\frac{3\lambda_2}{k_2^2}}exp\left\{\frac{3\lambda_2(1+k_2)(1+z)}{k_2^2(1+k_2+z)}\right\}}{\Omega_{rad,0}(1+z)^4 + \Omega_{m0}(1+z)^3 + \Omega_{\phi0}\,\beta\,(\frac{1+k_1+z}{1+z})^{-\frac{3\lambda_1}{k_1}}(\frac{1+k_2+z}{1+z})^{\frac{3\lambda_2}{k_2^2}}exp\left\{\frac{3\lambda_2(1+k_2)(1+z)}{k_2^2(1+k_2+z)}\right\}}$$

$$\times\left[\lambda_2\left(\frac{1+k_2+z}{1+z}\right)^{-1} - \lambda_2\,(1+k_2)\left(\frac{1+k_2+z}{1+z}\right)^{-2} - \lambda_1\left(\frac{1+k_1+z}{1+z}\right)^{-1}\right] \qquad . \tag{14}$$

To study the situation in every direction we analyse the density parameters for the matter field (Ω_m) and scalar field (Ω_ϕ) as,

$$\Omega_m(z) = \frac{\Omega_{m0}(1+z)^3}{\Omega_{rad,0}(1+z)^4 + \Omega_{m0}(1+z)^3 + \beta\,\Omega_{\phi0}\,(\frac{1+k_1+z}{1+z})^{-\frac{3\lambda_1}{k_1}}(\frac{1+k_2+z}{1+z})^{\frac{3\lambda_2}{k_2^2}}exp\left\{\frac{3\lambda_2(1+k_2)(1+z)}{k_2^2(1+k_2+z)}\right\}} \qquad . \tag{15}$$

and

$$\Omega_\phi(z) = \frac{\beta\,\Omega_{\phi0}\,(\frac{1+k_1+z}{1+z})^{-\frac{3\lambda_1}{k_1}}(\frac{1+k_2+z}{1+z})^{\frac{3\lambda_2}{k_2^2}}exp\left\{\frac{3\lambda_2(1+k_2)(1+z)}{k_2^2(1+k_2+z)}\right\}}{\Omega_{rad,0}(1+z)^4 + \Omega_{m0}(1+z)^3 + \beta\,\Omega_{\phi0}\,(\frac{1+k_1+z}{1+z})^{-\frac{3\lambda_1}{k_1}}(\frac{1+k_2+z}{1+z})^{\frac{3\lambda_2}{k_2^2}}exp\left\{\frac{3\lambda_2(1+k_2)(1+z)}{k_2^2(1+k_2+z)}\right\}} \qquad . \tag{16}$$

Now adding (3) and (4), we can obtain,

$$\dot{\phi}^2 = (1+z)^2 H^2\left(\frac{d\phi}{dz}\right)$$

$$\Rightarrow \frac{d\phi(z)}{dz} = \pm(1+z)^{-1}\sqrt{3}\left[\frac{\lambda}{1+k_1+z} + \frac{\lambda_2 z}{(1+k_2+z)^2}\right]^{\frac{1}{2}}$$

$$\times \left[1 + \frac{\Omega_{rad,0}(1+z)^4 + \Omega_{m0}(1+z)^3}{\Omega_{\phi 0}\beta\left(\frac{1+k_1+z}{1+z}\right)^{-\frac{3\lambda_1}{k_1}}\left(\frac{1+k_2+z}{1+z}\right)^{\frac{3\lambda_2}{k_2^2}}exp\left\{\frac{3\lambda_2(1+k_2)(1+z)}{k_2^2(1+k_2+z)}\right\}}\right]^{-\frac{1}{2}} \qquad . \qquad (17)$$

Again from equations (3) and (4), we can rewrite the potential in terms of that scalar field as,

$$V(\phi) = \frac{1}{2}\rho_\phi(1-\omega_\phi) \qquad . \qquad (18)$$

In terms of z, we can express $V(z)$ as

$$V(z) = V_0\left(\frac{1+k_1+z}{1+z}\right)^{-\frac{3\lambda_1}{k_1}}\left(\frac{1+k_2+z}{1+z}\right)^{\frac{3\lambda_2}{k_2^2}}exp\left\{\frac{3\lambda_2(1+k_2)(1+z)}{k_2^2(1+k_2+z)}\right\}\left(1-\frac{\lambda_1}{2(1+k_1+z)}-\frac{\lambda_2 z}{2(1+k_2+z)^2}\right) \qquad . $$
$$(19)$$

where , $V_0 = 3H_0^2\Omega_{\phi 0}\beta$.

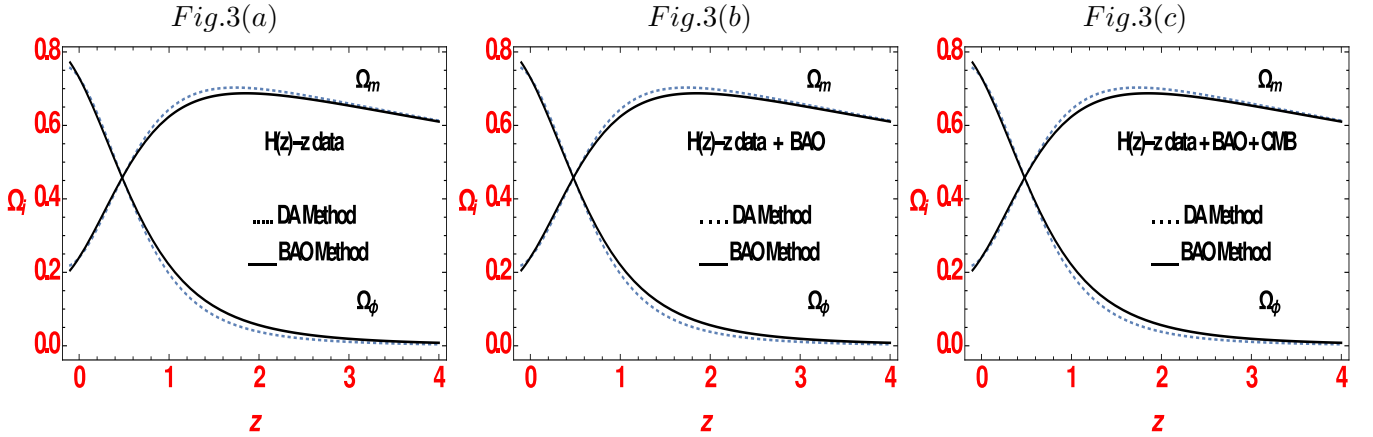

Fig.3(a)-(c) : Ω_m, Ω_ϕ vs z graphs, where dotted lines show DA method and solid lines show BAO method in the case of $H(z) - z$ data, $H(z) - z$ data with BAO, $H(z) - z$ data + BAO + CMB respectively.

In figure 3(a)-3(c) we have plotted the fractional dimensionless densities Ω_m for matter and Ω_ϕ for the exotic matter with respect to redshift z. In three of the cases ($H(z) - z$ data, $H(z) - z$ data+ BAO, $H(z) - z$ data + BAO + CMB) respectively. We observe that the fractional densities are of increasing nature in past with more or less same slope. $\Omega_m > \Omega_\phi$ for high z. But as time grows, Ω_ϕ increases and after a certain point, $z = z_1$ (say), Ω_ϕ turns greater than Ω_ϕ. These graphs, to some extent, supports the theory that in extreme part, the universe was matter dominated with $\Lambda = 0$. But as time grows, a delayed decay in matter world took place. This converted matter into relativistic hypothetical energy counterpart and finally $a = -1$ epoch came to exist at the present time. This theory [73, 74] even helped a lot to bypass different theoretical discrepancies faced by $\lambda = -1$ model alone. Fig 3(a)-(c) also depict that DA method is more appropriate than BAO to explain the transit from $\Lambda = 0$ to -1.

We plot q as a function of z in fig 4(a)-(c). q is found to be a decreasing function with time. The rate of q's contraction is low at high z and high at low z. We do not find any z where q changes its sign. So a transition from deceleration to acceleration is not allowed for our model. We find at least two $z(= z_2 and z_3)$. In other domains of z $q_{BAO}(z) > q_{DA}(z)$. The negativity of $q(z)$ is higher at $z = 0$ for DA method. This signifies high accelerated expansion is supported by DA method than BAO method.

In figure 5(a)-(c), we plot ω_ϕ vs z. The whole curve stays in negative zone/ fourth quadrant of $z - \omega_\phi$ plane. The value of ω_ϕ is decreasing for a region of high z. As z turns low, ω_ϕ starts to increase and its value becomes almost equal to -1 at a little past or a small neighbourhood of present time or $z = 0$

Fig 6(a)-(c) are plots of $\frac{d\omega_\phi}{dz}$ vs z. The rate of changes of ω_ϕ with respect to z increases in high z and then it falls near the present time.
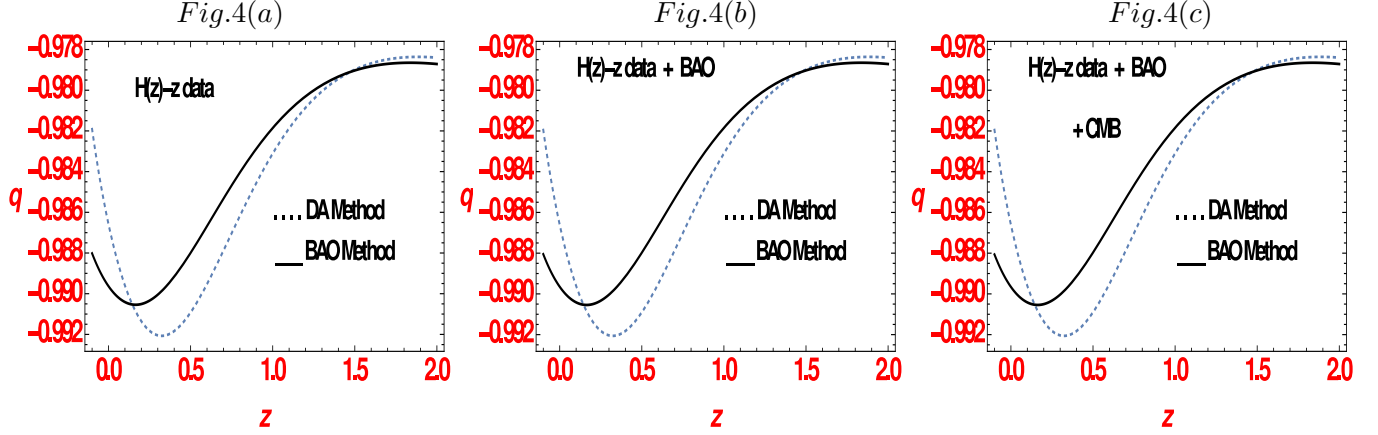
Fig.4(a)-(c) : q vs z graphs, where dotted lines are drawn for DA method and solid lines are drawn for BAO method. From fig 4(a) to 4(c) the graphs are for $H(z) - z$ data, $H(z) - z$ data + BAO and $H(z) - z$ data + BAO + CMB respectively.
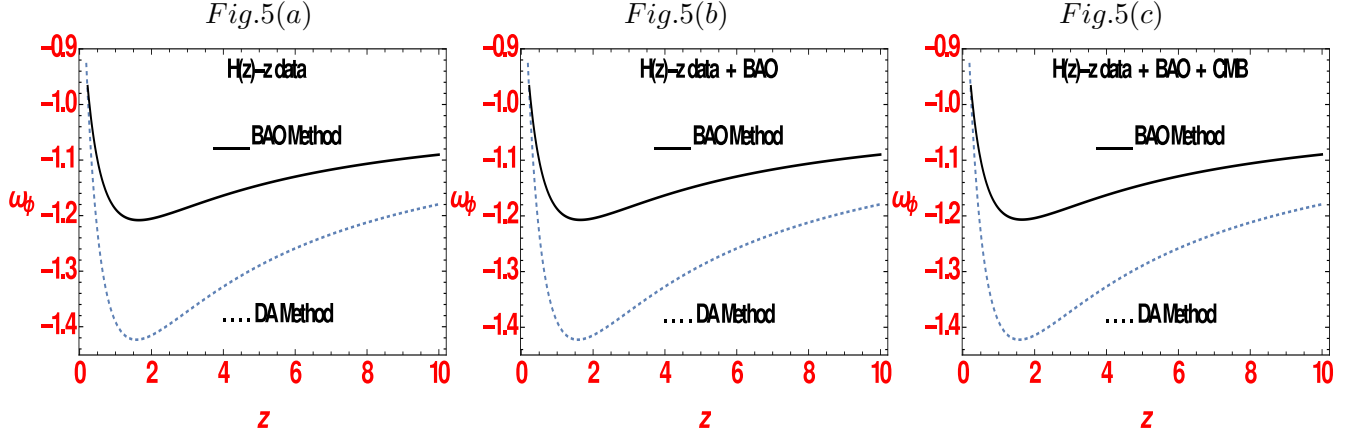

Fig.5(a)-(c) : Using $H(z) - z$ data, $H(z) - z$ data + BAO and $H(z) - z$ data with BAO +CMBω_ϕ vs z graphs, where dotted lines shows DA method and solid line shows BAO method.

5 Brief Discussions and Conclusions :

This article comprises of the construction of a redshift dependent model of dark energy and this model's behaviour under the constraints given by two particular redshift-Hubble parameter data sets. We have started with a cosmological model which is mainly governed by two independent components of Einstein's field equations for FLRW metric and equation of continuity for energy and matter. We have noticed that only three among these four governing equations can be independent of each other. But we were to solve four different quantities. This is why the requirement to consider a fourth is followed. This we have done by a process which gave birth of a new equation of state for the corresponding dark energy present in the current cosmos. As we have introduced a new dark energy representative, we require to specify the values of its different parameters. To do so we have motivated ourselves to constrain the parameters for two $H(z) - z$ data sets : derived from namely the differential ages method and Baryonic Acoustic Oscillation method. Firstly we plot these two data with each other and observe that the $H(z)$ graph is almost increasing with respect to corresponding z. The interesting part of this graph is that the higher values of $H(z)$ for low redshift can be seen in BAO case rather than DA method. The similar opposite phenomena happens for higher values of both redshift and $H(z)$ in DA method compared to BAO case. Next, we locate the best fit values of two parameters of our model under the data sets obtained by DA method and BAO method (along with BAO scaling and CMB constraints). We have plotted the 1σ, 2σ and 3σ confidence contours for both datasets. We have observed that the contours are elliptic type, the semi major axis of which is inclined with a slope greater than one right angle. Confidence contours for DA method is almost a superset of that for BAO method. So BAO method constrains the
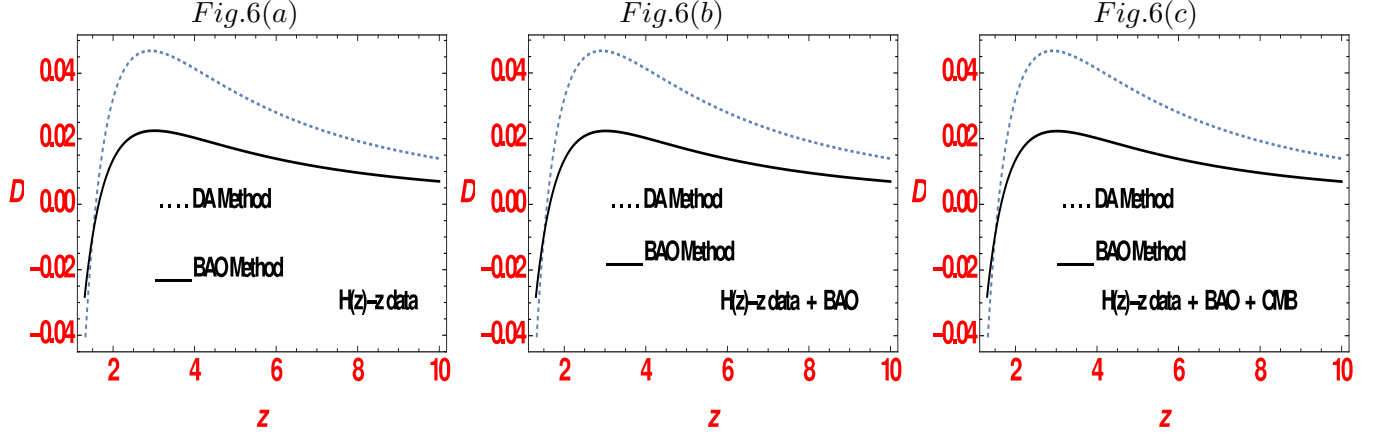
Fig.6(a)-(c) : Using $H(z) - z$ data, $D = \frac{d\omega_\phi}{dz}$ vs z graphs are drawn for $H(z) - z$ data, $H(z) - z$ data + BAO and $H(z) - z$ data + BAO + CMB respectively, where dotted lines describes DA method and solid line describes BAO method.

model more than DA method does. We have noted down the best its of the parameters λ_1 and λ_2 along with the span of the confidence contours in different tables. Fractional dimensionless densities for our model lies in the interval $[0, 1]$ and fractional density for dark energy increases with time. On the other hand, deceleration parameter's value decreases with time.

The interesting result is found when we check the variation of the equation of state parameter with redshift. EoS parameter decreases with time and then increases again to become equal to almost -1 at the pat neighbourhood of present time. From our model, we can theoretically construct the algebraic structure of the deceleration parameter, fraction dimensionless density, $\frac{d\omega_\phi(z)}{dz}$ etc. We have plotted them as well to understand the deeper insight.

Variations of fractional dimensional densities show quite interesting phenomena. We observe the fractional density of dark energy to start almost from zero at high z and to grow gradually. The same parameter for matter shows completely the opposite behaviour. For low redshift, the fractional density for dark energy grows high and almost becomes asymptotic to unity. This matches with a delayed decay of dark matter into dark energy with time.

Study of deceleration parameter vs redshift does not show any transition from deceleration to acceleration or converse. For present time neighbourhood q falls abruptly. Variation of $\omega(z)$ shows that at present epoch $\omega(z)$ is converging to -1, especially when $H(z) - z$ data + BAO + CMB is applied as constraining tool.

To conclude in brief, our model which is of inverse quadratic nature fits with $H(z)$ vs z data sets derived with the help of different ages method and Baryonic Acoustic Oscillation method by giving the best fits of the (λ_1, λ_2) type as (0.489817, -2.75048) and (0.282254, -1.4176) respectively. Both the data sets indicates to a $\omega \sim -1$ cosmology in $z = 0$ epoch. DA does it with a prompt jump than a slower slope of BAO. Probable decay from matter to energy in late time universe is noted.

References

[1] Supernova Search Team collaboration, Riess, A.G. et al. :- *" Observational evidence from supernovae for an accelerating universe and a cosmological constant" Astron. J.* **116** (1998) 1009 [astro-ph/9805201].

[2] Supernova Cosmology Project collaboration, Perlmutter, S. et al. :- *" Measurements of Ω and Λ from 42 high redshift supernovae" Astrophys. J.* **517** (1999) 565 [astro-ph/9812133].

[3] Einstein, A. :- *"Cosmological Considerations in the General Theory of Relativity."*; *Sitzungsber. Preuss. Akad. Wiss. Berlin (Math. Phys.),* **142** (1917).

[4] Zeldovich, Y.B. :- *" Special Issue: the Cosmological Constant and the Theory of Elementary Particles."*; *Soviet Physics Uspekhi* **11**, (1968) 381.

[5] Friedmann, A. :- *"On the curvature of space."* ; *Z. Phys.* **10**, (1922) 377.

[6] Lemaitre, G. :- *"Un Univers homogène de masse constante et de rayon croissant rendant compte de la vitesse radiale des nébuleuses extra-galactiques.*; *Annales de la Société Scientifique de Bruxelles* **47**, (1927) 49.

[7] Hubble, E. :- *"A relation between distance and radial velocity among extra–galactic nebulae."* *Proc. Nat. Acad. Sci.* **15**, (1929) 168.

[8] Bernardis, P. de et al.[Boomerang Collaboration] :- *A Flat Universe from High-Resolution Maps of the Cosmic Microwave Background Radiation"* ,*Nature* **404**, (2000) 955 [arXiv:0004404v1].

[9] Hanany, S. et al. :- *"MAXIMA-1: A Measurement of the Cosmic Microwave Background Anisotropy on angular scales of 10 arcminutes to 5 degrees"* , Astrophys. J. **545**, (2000) L5 [arXiv:0005123].

[10] Peebles, P. J. E. & Ratra, B. :- "The Cosmological Constant and Dark Energy" , *Rev. Mod. Phys.*, **75** (2003) 559 [arXiv:0207347v2].

[11] Biswas, P. & Biswas, R. :- *"Evolution of universe as a homogeneous system: Changes of scale factors with different dark energy Equation of States"* , *Modern Physics Letters A*, **33**, No. 19, (2018) 1850106 [arXiv:1710.06307].

[12] Sahni, V., Starobinsky, A. A. :- *"The Case for a Positive Cosmological Lambda-term"* , *Int. J. Mod. Phys. D*, **9** (2000) 373 [arXiv:9904398v2].

[13] Ozer, M., Taha, M. O. :- *"A possible solution to the main cosmological problems"* , *Phys. Lett. B*, **171** (1986) 363.

[14] Biswas, P. & Biswas, R. :- *"Interacting Models of Generalized Chaplygin Gas and Modified Chaplygin Gas with Barotropic Fluid"* , *Modern Physics Letters A*, [arXiv:1805.03962].

[15] Biswas, R. & Debnath, U. :- *"Constraining redshift parametrization parameters of dark energy: loop quantum gravity as background"* , *Eur.Phys.J.C*, **73** (2013) no.5, 2424.

[16] Biswas,P. & Biswas, R :- *"Barboza-Alcaniz Equation of State Parametrization : Constraining the Parameters in Different Gravity Theories"* , (2018) [arXiv:1807.10608].

[17] Ratra, B., Peebles, P.J.E.:- *"Cosmological consequences of a rolling homogeneous scalar field"* , *Phys. Rev. D* **37**, (1988) 3406.

[18] Linder, E.V. :- *"Cosmic growth history and expansion history"* , *Phys. Rev. D* **72**, (2005) 043529 [arXiv:0507263].

[19] Wang, X. et al.:- *" Observational constraints on cosmic neutrinos and dark energy revisited"*, *JCAP* **11** (2012) 018 [arXiv:1210.2136].

[20] Linder, E.V. :- *"Exploring the Expansion History of the Universe"* , *Phys. Rev. Lett.*, **90** (2003) 091301 [arXiv:0208512v1].

[21] Pan, Z., Knox, L., Mulroe, B. & Narimani, A. :- *"Cosmic Microwave Background Acoustic Peak Locations"* , *MNRAS*, **459** (2016) 2515 [arXiv:1603.03091v2].

[22] Bassett, B. A. & Hlozek, R. :- *"Baryon Acoustic Oscillations"* , *Dark Energy, Ed. P. Ruiz-Lapuente*, (2010) [arXiv:0910.5224v1].

[23] Copeland, E. J., Sami, M. & Tsujikawa, S. :- *"Dynamics of dark energy"* , *Int. J. Mod. Phys. D* , **15** (2006) 1753 [arXiv:0603057v3].

[24] SDSS collaboration, Eisenstein, D. J. et al. :- *"Detection of the baryon acoustic peak in the large-scale correlation function of SDSS luminous red galaxies"* , *Astrophys. J.*, **633** (2005) 560 [arXiv:0501171].

[25] Cole, S. et al. :- *"The 2dF Galaxy Redshift Survey: power-spectrum analysis of the final data set and cosmological implications"* , *Mon. Not. Roy. Astron. Soc.*, **362** (2005) 505 [arXiv:0501174].

[26] Planck collaboration, Ade, P. A. R. et al. :- *"Planck 2015 results. XIII. Cosmological parameters"* , [arXiv:1502.01589].

[27] Jimenez, R. & Loeb, A. :- *"Constraining cosmological parameters based on relative galaxy ages"* , *Astrophys. J.*, **573** (2002) 37 [arXiv:astro-ph/0106145].

[28] Valent, A. G. & Amendola, L. :- *"H_0 from cosmic chronometers and Type Ia supernovae, with Gaussian Processes and the novel Weighted Polynomial Regression method"* , *JCAP*, **1804** (2018) 051, [arXiv:2.01505v3].

[29] Moresco, M. et al. :- *"Improved constraints on the expansion rate of the Universe up to $z \sim 1.1$ from the spectroscopic evolution of cosmic chronometers"* , *JCAP*, **08** (2012) 006 [arXiv:1201.3609].

[30] Moresco, M., Verde, L., Pozzetti, L., Jimenez, R. & Cimatti, A. :- *"New constraints on cosmological parameters and neutrino properties using the expansion rate of the Universe to $z \sim 1.75$"* , *JCAP*, **07** (2012) 053 [arXiv:1201.6658].

[31] Zhao, G. -B., Crittenden, R. G., Pogosian, L.& Zhang, X. :- *"Examining the evidence for dynamical dark energy"* , *Phys. Rev. Lett.*, **109** (2012) 171301 [arXiv:1207.3804].

[32] Riemer-Sorensen, S., Parkinson, D., Davis, T. M. & Blake, C. :- *"Simultaneous constraints on the number and mass of relativistic species"* , *Astrophys. J.*, **763** (2013) 89 [arXiv:1210.2131].

[33] Moresco, M. et al. :- *"A 6% measurement of the Hubble parameter at $z \sim 0.45$: direct evidence of the epoch of cosmic re-acceleration"* , *JCAP*, **05** (2016) 014 [arXiv:1601.01701v2].

[34] Jimenez, R., Verde, L., Treu, T. and Stern, D. :- *"Constraints on the equation of state of dark energy and the Hubble constant from stellar ages and the cosmic microwave background"*, *Astrophys. J*, **593**, (2003) 622–629, [arXiv:0302560].

[35] McCarthy, P. J. et al :- *"Evolved galaxies at $z > 1.5$ fromthe Gemini Deep Deep Survey: The formation epoch of massive stellar systems"*, *Astrophys. J*, **614** ,(2004) L9–L12, [arXiv:0408367].

[36] Jimenez, R. et al :- *"Premature dismissal of high-redshift elliptical galaxies"*, *Mon. Not. R. Astron. Soc.*, **305**, (1999) L16–L20 , [arXiv:9812222].

[37] Dunlop, J., Peacock, J., Spinrad, H., Dey, A., Jimenez, R., Stern, D., & Windhorst, R. :- *"A 3.5-Gyr-old galaxy at redshift 1.55"*, *Nature*, **381**, 581 (1996).

[38] Alcaniz, J. S. & Lima, J. A. S. :- *"Dark Energy And The Epoch Of Galaxy Formation" ApJ*, **550**, L133 (2001).

[39] Stockton, A. :- *"The Oldest Stellar Populations at $z \sim 1.5$"*, to be published in Astrophysical Ages and Time Scales, ASP Conference Series, (2001) [arXiv:0104191].

[40] Macaulay, E. et. al. (DES collaboration) :- *"First Cosmological Results using Type Ia Supernovae from the Dark Energy Survey: Measurement of the Hubble Constant"* , [arXiv:1811.02376].

[41] Zhang, C., Zhang, H., Yuan, S., Zhang, T. -J. & Sun, Y. -C. :- *"Four new observational $H(z)$ data from luminous red galaxies in the Sloan Digital Sky Survey data release seven"* , *Res. Astron. Astrophys.*, **14**, 1221 (2014) [arXiv:1207.4541].

[42] Simon, J., Verde, L. & Jimenez, R. :- *"Constraints on the redshift dependence of the dark energy potential"* , *Phys. Rev. D*, **71** 123001 (2005) [arXiv:0412269].

[43] Stern, D. et al. :- *"Cosmic chronometers: constraining the equation of state of dark energy. I: $H(z)$ measurements"* , *JCAP*, **1002** (2010) 008 [arXiv:0907.3149].

[44] E. Gazta ñaga, A. Cabr e\ and L. Hui :- *"Clustering of luminous red galaxies - IV. Baryonacoustic peak in the line-of-sight direction and a direct measurement of $H(z)$"* , *Mon. Not. R.Astron. Soc.*, **399** (2009) 1663 [arXiv:0807.3551]

[45] Chuang, C. H. & Wang, Y., :- "Modeling the anisotropic two-point galaxy correlation function on small scales and improved measurements of $H(z)$ from the Sloan Digital Sky Survey DR7 luminous red galaxies" , *Mon. Not. R. Astron. Soc*, **435** (2013) 255 [arXiv:1209.0210].

[46] Alam, S., et al. :- *"The clustering of galaxies in the completed SDSS-III Baryon Oscillation Spectroscopic Survey: cosmological analysis of the DR12 galaxy sample"* , (2016), [arXiv:1607.03155]

[47] Blake, C. et al. :- *"The WiggleZ Dark Energy Survey: joint measurements of the expansion and growth history at $z \leq 1$."* , *Mon. Not. R. Astron. Soc*, **425** (2012) 405 [arXiv:1204.3674].

[48] Ratsimbazafy, A. L. et al. :- *"Age–dating Luminous Red Galaxies observed with the Southern African Large Telescope"* , *Mon. Not. Roy. Astron. Soc.*, **467** (2017) 3239 [arXiv:1702.00418].

[49] Anderson, L. et al. [BOSS Collaboration] :- *"The clustering of galaxies in the SDSS-III Baryon Oscillation Spectroscopic Survey: baryon acoustic oscillations in the Data Releases 10 and 11 Galaxy samples."* , *Mon. Not. R. Astron. Soc*, **441(1)** (2014) 24 [arXiv:1312.4877].

[50] Moresco, M. :- *"Raising the bar: new constraints on the Hubble parameter with cosmic chronometers at $z \sim 2$"* , *Mon. Not. Roy. Astron. Soc.*, **450** (2015) L16 [arXiv:1503.01116].

[51] N. G. Busca, T. Delubac, J. Rich, et al. :- *"Baryon acoustic oscillations in the Ly alpha forest of BOSS quasars"* , *Astron. & Astrophys.*, **552** (2013) 18 [arXiv:1211.2616].

[52] Delubac , T. et al. [BOSS Collaboration], *"Baryon acoustic oscillations in the L_y forest of BOSS DR11 quasars"* , *Astron. Astrophys.*, **574** (2015) A59 [arXiv:1404.1801].

[53] Font-Ribera, A., et al. :- *"Quasar-Lyman α Forest Cross-Correlation from BOSS DR11 : Baryon Acoustic Oscillations"* , *JCAP*, **1405**, (2014) 027 [arXiv:1311.1767].

[54] Oka A. et al.:- *"Simultaneous constraints on the growth of structure and cosmic expansion from the multipole power spectra of the SDSS DR7 LRG sample"* , *Mon. Not. Roy. Astron. Soc.*, **439**, (2014) 2515-2530 [arXiv: 1310.2820].

[55] Wang Y. et al. :- *"The clustering of galaxies in the completed SDSS-III BaryonOscillation SpectroscopicSurvey: tomographic BAO analysis of DR12 combined sample configuration space* , *Mon. Not. Roy.Astron. Soc.*, **469**, (2017) 3762–3774 [arXiv:1607.03154].

[56] Chuang C.H. and Wang Y. *"Modeling the Anisotropic Two-Point Galaxy Correlation Function on SmallScales and Improved Measurements of $H(z)$, $DA(z)$, and $f(z)\,\sigma 8(z)$ from the Sloan Digital Sky Survey DR7 Luminous Red Galaxies"* , *Mon. Not. Roy. Astron. Soc.*, **435**, (2013) 255-262 [arXiv:1209.0210].

[57] Chuang C-H. et al. *"The clustering of galaxies in the SDSS-III Baryon Oscillation Spectroscopic Survey : single-probe measurements and the strong power of $f(z)\sigma 8(z)$ on constraining dark energy"* , *Mon. Not.Roy. Astron. Soc.*, **433**, (2013). 3559-3571 [arXiv:1303.4486].

[58] Bautista J. E. et al. :- *"Measurement of baryon acoustic oscillation correlations at $z = 2.3$ with SDSSDR12 $L_{y\alpha}$-Forests"* ,*Astron. Astrophys.*,**603**, (2017) 23 [arXiv:1702.00176].

[59] Barboza Jr., E. M., Alcaniz, J. S. :- *"A parametric model for dark energy"* , *Phys. Lett. B*, **666**, (2008) 415 [arXiv:0805.1713v1].

[60] Efstathiou, G. :- *"Constraining the equation of state of the Universe from Distant Type Ia Supernovae and Cosmic Microwave Background Anisotropies"* , *Mon. Not. R. Astron. Soc.*, **310**, (1999) 842 [arXiv:9904356v1].

[61] Silva, R., Alcaniz J. S. and Lima, J. A. S. :- it *"On the thermodynamics of dark energy"* , *Int. J. Mod. Phys. D* **16**, (2007) 469.

[62] Alam, U., Sahni, V., Saini, T. D., Starobinski, A. A. :- *"Is there supernova evidence for dark energy metamorphosis?"* , *Mon. Not. R. Astron. Soc.*, **354** (2004a) 275 [arXiv:0311364].

[63] Alam, U., Sahni, V., Starobinski, A. A. :- *"The case for dynamical dark energy revisited"* , *JCAP*, **0406**, (2004b) 008 [arXiv:0403687v2].

[64] Hannestad, S., Mörtsell, E. :- *"Cosmological constraints on the dark energy equation of state and its evolution"*, **JCAP**, **0409**, (2004) 001, [arXiv:0407259].

[65] Lee, S., :- *"Constraints on the dark energy equation of state from the separation of CMB peaks and the evolution of alpha "*, **Phys. Rev. D**, **71**, (2005) 123528 [arXiv:0504650].

[66] Feng, C., J., Shen, X. -Y., Li, P., Li, X. -Z., :- *A New Class of Parametrization for Dark Energy without Divergence"* , **JCAP**, **1209**, (2012) 023, [arXiv:1206.0063].

[67] Weller, J., Albrecht, A., :- *"Future supernova observations as a probe of dark energy"* , **Phys. Rev. D**, **65**, (2002) 103512 [arXiv:0106079].

[68] Sendra, I., Lazkoz, R., :- *"SN and BAO constraints on (new) polynomial dark energy parametrizations: current results and forecasts"* , **Mon. Not. Roy. Astron. Soc.**, **422**, (2012) 776 [arXiv:1105.4943].

[69] Lima, J. A. S., Alcaniz, J. S. :- *"Flat FRW Cosmologies with Adiabatic Matter Creation: Kinematic tests"* , *Astron. Astrophys.*, **348**, (1999) 1 [arxiv:9902337].

[70] Doran, M., Stern. S, and Thommes, E. :- *"Baryon acoustic oscillations and dynamical dark energy"* , *JCAP*, **0704**, (2007) 015 [arXiv:0609075].

[71] Elgaroy, O. and Multamaki, T. :- *"On using the cosmic microwave background shift parameter in tests of models of dark energy"* , *Astron. Astrophys*, **471** (2007) 65E [arXiv:0702343].

[72] Efstathiou, G. and Bond J. R. :- *"Cosmic confusion: degeneracies among cosmological parameters derived from measurements of microwave background anisotropies"* , *MNRAS*, **304**, (1999) 75 [arXiv:9807103].

[73] Turner, M. S., Steigman, G. & Krauss, L. M. :- *"Flatness of the Universe: Reconciling Theoretical Prejudices with Observational Data"* , *Phys. Rev.Lett.*, **52**, (1984) 2090.

[74] Mathews, G. J., Lan, N. Q. & Kolda, C. :- *"Late decaying dark matter, bulk viscosity, and the cosmic acceleration"* , *Phys. Rev. D*, **78**, (2008) 043525 [arXiv:0801.0853].